Cytokine Profile and Glial Activation Following Brachial Plexus Roots Avulsion Injury in Mice

Ke Zhong
Sun Yat-sen University Zhongshan School of Medicine https://orcid.org/0000-0001-8666-7102
Yinqin Li
Fifth Affiliated Hospital of Sun Yat-sen University
Ying Tang
Sun Yat-sen University Zhongshan School of Medicine
Guangying Yu
Sun Yat-sen University Zhongshan School of Medicine
PRINCE LAST MUDENDA ZILUNDU
Sun Yat-sen University Zhongshan School of Medicine
Yingying Zhou
Sun Yat-sen University Zhongshan School of Medicine
Xiaoying Xu
Sun Yat-sen University Zhongshan School of Medicine
Rao Fu
School of Medicine(Shenzhen), Sun Yat-sen University
Lihua Zhou (zhoulih@mail.sysu.edu.cn)
https://orcid.org/0000-0003-2516-2463

Research

Keywords: cytokine profile, nerve injury, motoneuron degeneration, mice

DOI: https://doi.org/10.21203/rs.3.rs-27602/v1

Abstract

Background Inflammation and tissue infiltration by various immune cells play a significant role in the pathogenesis of neurons suffering the central nervous systems diseases. Although brachial plexus root avulsion (BPRA) leads to dramatic motoneurons (MNs) death and permanent loss of function, however, the crosstalk between cytokines and glial reaction in the spinal cord during injury is far beyond our knowledge. The current study is sought to investigate the alteration of specific cytokine expression patterns of BPRA injured spinal cord during an acute and subacute period.

Methods Here, cytokine assay, transmission electron microscopy, and histological staining were utilized to assess the alteration of cytokine network, ultrastructure morphology, as well as glial activation and loss of MNs within two weeks, post-injury on a mouse BPRA model.

Results We found that BPRA significantly changed the level of CXCL1, IL12 p70, ICAM1, IP10, MCP-5, MIP1-α and CD93. Moreover, the elevated MIP1-α and CD93 were mostly distributed in MNs of the injured, but few in healthy segments. Also, BPRA significantly induced glial reactions in the ventral horn of injured spinal segments, reflected by robustly elevated the Ionized calcium-binding adaptor molecule 1 (IBA1) and Glial fibrillary acidic protein (GFAP) positive cells. We also observed a severe progressively loss of injured MNs, with a character of both apoptosis and necrosis.

Conclusion Overall, these findings suggested that the inflammatory cytokines associated with glial cell proliferation play a vital role in the pathophysiology of MNs death caused by nerve roots injury.

Background

Motoneurons (MNs) degenerate progressively and finally die after the brachial plexus root avulsion (BPRA), an injury-causing paralysis of the target muscle groups of the upper limbs [1][2]. Neuroinflammation is one of the essential factors for triggering the neuron loss related to acute or chronic neurodegenerative disorders [3]. It has been well documented that the neuroinflammation also plays a causal role for the MNs degeneration and death associated with spinal cord injury, including avulsion injury [4][5][6][7].

It has been reported that the neuroinflammation is characteristic of the infiltration of leukocytes [8] and glial activation during the acute and subacute period after spinal cord injury [9] [10][11].

The inflammation of BPRA is attributed to that lesion created cellular debris, which activates the astrocytes and microglia, trigging the release of a wide variety of oxidative stress regulators, growth factors, and inflammatory mediators including cytokines[12]. The cytokines are proteins that coordinate the immune response throughout the CNS, recruiting phagocytic cells, like peripheral neutrophils and macrophages into the injured spinal cord [13][14], which are considered to be the first wave of infiltrating immune cells [15].

On one side, cytokines have shown a role in debris clearance, cellular remodeling, and production of pro-regenerative factors[16][17] [18][19]. For example, Several studies reported the level of anti-inflammatory cytokines, like interleukin 4 (IL-4), interleukin 10 (IL-10) and transforming growth factor-β (TGF-β), substantially enhanced after undergoing post-spinal cord injury activation by injured neurons and astrocyte[20] [21][22]. However, other studies demonstrated that either microglia or astrocytes also produce pro-inflammatory cytokines such as interleukin 1 (IL-1), interleukin 6 (IL-6) and tumor necrosis factor α (TNF-α) during spinal cord injury [23][24][25], which suggest that cytokines are detrimental to CNS neurons [26] [27] and targets for the treatment of spinal cord injury [28][29][30][31].

The current study is sought to investigate how the alteration of specific cytokines expression patterns affects spinal glial activation and MNs death induced by BPRA. We observed that substantially elevated glial reactions and enhanced levels of cytokines, especially MIP-1α, which might contribute to a progressively MNs loss in the ventral horn of injured spinal segments caused by avulsion injury.

Methods

Animals

Experiments were conducted on 76 adult male C57BL/6 mice, 8–10 weeks old, weighing 20–25 g, which were purchased from the Laboratory Animal Center of Sun Yat-sen University (Guangzhou, China). The number of the animal use permit is SYXK 2017-0081. The mice were housed under a 12-hour light/dark cycle with food and water were available ad libitum. Surgical and animal care procedures were carried out under the provisions outlined in the National Health and Medical Research Council animal ethics and ARRIVE guidelines. All procedures were performed with the approval of the Animal Care and Utilization Committee of Sun Yat-sen University.

Animal Model Setting

The microsurgery procedure for the brachial plexus roots avulsion injury was as we described previously [32][33][34][35].In short, the mice were under anesthesia induced with ketamine/xylazine (80/20 mg/kg, i.p.) and maintained with 1% isoflurane. With each mouse in the supine position, the right side of brachial plexus was exposed, and its C5- T1 spinal nerve roots were separated under a surgical microscope (ChengHe Microsurgical Instruments Factory, Ning Bo, China). Both dorsal and ventral rootlets were pulled out using micro hemostatic forceps. All the avulsed distal parts of roots were cut away, and the success of the avulsion model confirmed under the microscope. The muscle and skin were sutured in successive layers. The mice were placed in a heated recovery chamber until they were fully awake and then returned to their cages.

Tissue Preparation

To assess the spinal cord cytokines profile of BPRA mice, a serial of time points [1, 2, 3, 5, 7 and 14 day post injury (dpi)], mice were anesthetized with 1% sodium pentobarbital (40 mg/kg, i.p., Sigma-Aldrich) and the cervical spinal cord was exposed by laminectomy under the surgical microscope. Subsequently, the C5 to T1 spinal segments were quickly removed and immediately divided into ipsilateral and contralateral halves. Spinal cord tissues were frozen in liquid nitrogen for subsequent protein extract. The frozen samples were homogenized in Whole-Cell Lysis buffer (KGP2100, Key GEN Biotech. Co., Ltd. Nanjing, China) containing protease inhibitor and 1 mM PMSF (P7626; Sigma-Aldrich, St. Louis, Missouri) using an electric homogenizer. The homogenates were lysed in ice for 1 h and centrifuged at 12,000 rpm for 30 min at 4 °C. The supernatants were collected, and the protein concentrations were measured using the BCA (SL260619, Thermo Scientific; Rockford, Illinois) method and stored at − 80 °C until the time of cytokine measurement.

Cytokine Assay

Spinal cord samples (n = 6 mice/group for each time point) were evaluated using the 20-plex, Mouse Premixed Multi-Analyte Kit LXSASM-20 (L126405, R&D Systems, Minneapolis, MN), measured with the Luminex system (Luminex, Austin, TX), and analyzed by Bio-plex software (Bio-Rad, Hercules, CA). This panel includes: C-X-C motif chemokine ligand 1(CXCL1), tumor necrosis factor-alpha (TNF-alpha), IL-12 p70, C-C motif chemokine 2 (CCL2), IL-1beta (IL-1b), IL-2, IL-6, IL-10, IL-17A, Intercellular adhesion molecule 1(ICAM-1), C-X-C motif chemokine 10 (IP-10), regulated on activation, normal T expressed and secreted protein (RANTES), C-C motif chemokine 12(CCL12), Beta-nerve growth factor (NGFb), macrophage inflammatory protein (MIP)-1alpha (MIP1-α), interleukin (IL)-alpha (IL-1a), Stromal cell-derived factor 1(SDF-1a,), Complement component C1q receptor(CD93), C-C motif chemokine 22(CCL22).

Immunofluorescence, Neutral Red Staining And Cell Counting

Twenty BPRA mice were sacrificed using a lethal dose of 1% sodium pentobarbital on the 1, 3, 7, and 14 dpi, respectively (n = 5/group at each time point). They were transcardially perfused with normal saline followed by cold 4% paraformaldehyde (PFA) in 0.1 M phosphate buffer (PB, pH 7.4). The cervical spinal cord was exposed by laminectomy under the surgical microscope. The C7-C8 spinal segments, which were defined as the region between the uppermost and the lowermost rootlets of the contralateral C7-C8 spinal nerves, were post-fixed by immersion in 4% PFA followed by overnight immersion in 30% (v/v) sucrose in PB solution at 4 °C. The transverse sections of the C7-C8 spinal cord (30 μm), were collected in 0.01M PBS. Every third section of the spinal cord was used for staining study.

The immunofluorescence (IF) was evaluated under a fluorescence microscope (BX63, Olympus, Japan). The sections were rinsed three times in PBS and then treated with 0.3% Triton X-100 and 0.1% bovine serum albumin (BSA) in PBS at room temperature for 30 min. The following primary antibodies were

used: mouse anti-NeuN antibody (1:500 dilution, ab104224, Abcam, UK), rabbit anti-GFAP (1:500 dilution; 80788S, CST, Danvers, Massachusetts), rabbit anti-IBA1 (1:500 dilution; 019-19741, Wako Bioproducts, Richmond, Virginia), rabbit anti-CD93 (1:200 dilution; ab198854 Abcam, UK), and rabbit anti-MIP1-α (1:100 dilution, ab25128, Abcam, UK). Incubation was at 4 °C overnight. Then, following washing three times with PBS, the sections were incubated with respective secondary antibodies. The following antibodies were used: Goat anti-Mouse IgG (H + L) Cross-Adsorbed Secondary Antibody, Alexa Fluor 488 (1:1500, A32723, Invitrogen, USA), Goat anti-Rabbit IgG (H + L) Cross-Adsorbed Secondary Antibody, Alexa Fluor 555 (1:1000, A32731, Invitrogen, USA). Incubation was 2 h at room temperature in the dark. After rinsing the sections three times with PBS, then incubated with Hoechst33342 (H3570, Life Technologies, USA). They were visualized under a fluorescence microscope. Staining without primary or secondary antibodies served as negative controls.

In addition, the neutral red staining was performed in C7 and C8 segments to assess MNs survival as previously reported [36][37]. Briefly, Sections were stained with 1% neutral red (N4638, Sigma-Aldrich, USA) in 0.1M acetic acid (pH4.8) for 2 h followed by dehydration in ethanol. Images were captured using a digital camera attached to the microscope. Next, the quantification of cell counting on the ventral horns of the both sides spinal cord (C7-C8 segments Rexed's lamina IX) was as described previously [38]. We computed the mean number of either IF or neural red positive cells from the total 7 ~ 8 sections obtained from each mouse. Only those neurons with both the nucleolus in the nucleus and Nissl bodies in the cytoplasm stained with neutral red we recounted under a 20 × objective lens. Two independent persons blinded to the sidedness of the groups performed cell counting, pooling of means and data analysis.

Transmission Electron Microscopy

Transmission electron microscopy (TEM) was used to assess motor neuron morphology in the spinal cord after BPRA at 1, 3, 7, 14 dpi (n = 5 mice/group at each time point). The mouse was perfused transcardially with 0.9% normal saline, followed by a mixture of 2% PFA and 2.5% glutaraldehyde (Sigma-Aldrich, G6257, USA) in 0.1 M PBS. Approximately 1 mm^3 of tissue per mice was dissected from the spinal cord and fixed in 2% glutaraldehyde for 2 h at 4 °C. The tissues were rinsed in 0.1 M cacodylate buffer and post-fixed with 1% osmium tetroxide for 2 h. Then, the tissue was rinsed with distilled water before undergoing dehydration in a graded ethanol series. Subsequently, the tissue was infiltrated overnight at 4 °C using a mixture of half acetone and half resin. The tissue was embedded in resin 24 h later and then cured fully as follows: 37 °C overnight, 45 °C for 12 h, and 60 °C for 24 h. After that, 70-nm sections were cut and stained with 3% uranyl acetate for 20 min and 0.5% lead citrate for 5 min. Ultrastructural changes motor neuron morphology was observed under TEM.

Statistical Analysis

All data were expressed as mean ± SEM (standard error of the mean). The morphological evaluation result or cytokine assay result was subjected to one-way or two-way measures ANOVA followed by a

Bonferroni or Tukey post hoc test for multiple group comparisons. A value of $p < 0.05$ was considered statistically significant.

Results

BPRA substantially caused MNs loss in the ventral horn of the injured spinal cord

At 1 dpi, the injured MNs started to present morphological features of both apoptosis and necrosis, reflected by slightly swollen mitochondria and condensed cytoplasm with a still visible nucleus and nucleolus. By 3–7 dpi, the cytoplasm of MNs had become hyperchromatic, the nuclear envelope was indistinct and irregular in shape, and the nucleoli and nuclei were more condensed. The cytoplasm also contained fragmented organelles, numerous, small, granular profiles and organelles are significantly reduced in the cytoplasm. Mitochondria were absent, and the cell membrane was disrupted (Fig. 1).

Moreover, the light microscopic observation also revealed an increase in the size of the cytoplasm of injured MNs. Furthermore, the neural red positive staining cell counting of spinal ventral horn found a significant and progressive decline in the ipsilateral MNs survival rate ($F_{(3,16)} = 674.3$, $p < 0.0001$), with only 35.34%± 0.48% ipsilateral MNs survived as compared to contralateral side at 14 dpi (Fig. 2).

BPRA enhance the glial activation in the ventral horn of the injured spinal cord

To evaluate the glial reactions that occurred in the injured spinal cord after BPRA, the expression of IBA-1 and GFAP, markers of activated microglia and astrocytes, were determined using immunoreactivity 1 to 14 dpi in both ipsilateral and contralateral side of the spinal ventral horn. Our results showed both IBA-1 average fluorescence intensity (AFI) and immunoreactivity (IR)-positive cells number of ipsilateral ventral horn gradually increased compared to the contralateral side within 1–14 days followed injury (AFI: $F_{(3,16)} = 487.7$, $p < 0.0001$; IR cell number, $F_{(3,16)} = 249.9$, $p < 0.0001$, Fig. 3). Similarly, we observed a robustly elevated GFAP expression trend in the

injured ventral horn after BPRA. Compared to the contralateral side, BPRA caused an increase in GFAP AFI ($F_{(3,16)} = 85.06$, $p < 0.0001$) and IR cell number ($F_{(3,16)} = 52.7$, $p < 0.0001$) in the ipsilateral side, with the peaks at 7 dpi (Fig. 4). These data suggested that BPRA produced microglia and glial activation in the injured spinal cord.

Discussion

The present study showed that BPRA substantially caused MNs loss in the ventral horn of the injured spinal cord. The damaged MNs is morphologically characteristic of swelling and depletion of mitochondria endoplasmic reticulum, and eventual rupture of organelles, and disruption of nuclear and plasma membranes. These changes are associated with glial activation in the affected ventral horn, reflected by enhanced IBA-1 and GFAP immunoreactivity. Moreover, we also found that some essential cytokines level substantially changed during the acute and subacute phase of MNs death, especially like MIP1-α and CD93 expression increased in the inured MNs. These data strongly suggest that cytokines might have crosstalk with glial activation, which contributes to the spinal MNs loss caused by avulsion injury.

Our study the changes of cytokine profile following BPRA (acute and subacute periods) in mice compared with contralateral ventral horns in the same injured spinal segments. During the first 2 weeks after BPRA, we detected significant changes in concentrations of 7 cytokines with different inflammatory and immunological activities. We found CXCL1 showed a rapidly enhanced concentration on 1 dpi then decreased to the baseline during 2–14 dpi. CXCL1, being a chemotactic substance for neutrophils, is expressed by macrophages, neutrophils, astrocytes and epithelial cells [40]. Studies in mice have shown that CXCL1 reduces the severity of multiple sclerosis and can exhibit a neuroprotective function. The concurrence of CXCR2(the receptor for CXCL1) on oligodendrocytes and induced CXCL1 on hypertrophic astrocytes in MS provides a novel mechanism for recruitment of oligodendrocytes to areas of damage, an essential prerequisite for lesion repair in this devastating condition. [41][42]. CXCL1 of might be actively involved in the regenerative processes by recruiting oligodendrocytes to the injured spinal cord on the first 1 day after BPRA.

On 2 dpi, we observed a reduced concentration of IL-12 p70 and maintained a relatively low level as compared to 1 dpi. Interleukin-12 (IL-12) is a heterodimeric cytokine produced mostly by phagocytic cells in response to bacteria, bacterial products, and intracellular parasites, and to some degree by B lymphocytes. The early preference expressed in the immune response depends on the balance between IL-12, which favors Thl responses, and IL-4, which favors Th2 responses. Thus,IL-12 represents a functional bridge between the early nonspecific innate resistance and the subsequent antigen-specific adaptive immunity [43].

Pro-inflammatory cytokine IP10 peaked at 1 dpi with a second peak at 14 dpi compared to the contralateral side of the spinal cord, which is secreted by several cell types (e.g., leukocytes, macrophages and endothelial cells) in response to IFN-γ and recruits these cells to sites of infection or inflammation after binding to C-X-C motif receptor (CXCR3) [44][45]. IP10 is expressed at low levels in the spinal cord under normal conditions, but upon stimulation, the expression of this chemokine is substantially increased at sites where glial cells accumulate [45]. Previous study found the neutralization of CXCR3 significantly reduces the expression of markers of activated microglia and astrocytes as well as the levels of proinflammatory cytokines and chemokines, such as CCL2 and CXCL10 [45][46][47].

Changes in the level of pro-inflammatory cytokine MCP5 in the form of a sharp increase in its level on 1 dpi were observed in injured spinal cord and maintained a relatively high level as compared to the contralateral side till 14 dpi. The cytokine MCP5 attracts eosinophils, monocytes, and lymphocytes but not neutrophils. Previous study found sequence analyses identified HIF-1α binding sites in the promoters of MCP-5 genes and HIF-1α is involved in transcriptional induction of MCP5 in astrocytes by hypoxia [48].

We found the pro-inflammatory chemokine MIP-1 α during the first 2 weeks after BPRA with a maximum increase of 13.94 times on 1 dpi, being a macrophage inflammation protein, activates granulocytes, which leads to acute neuroinflammation [49]. Immunofluorescence staining found MIP-1 α mostly located in the injured motor neuron after BPRA. Its increase in the spinal cord tissues may be associated with disruption of the blood–brain barrier and an increased migration of macrophages and neutrophils to the site of injury. Previous studies have shown the importance of MIP-1α in demyelination in the CNS and highlight its effect by exposing MIP-1α knockout mice (MIP-1α-/-) to cuprizone and comparing pathology to wild-type mice, which found demyelination was significantly decreased in MIP-1α-/- mice (near 36% reduction) [50]. We speculate that the high expression of MIP-1α may be related to attract macrophages infiltration and demyelination of motor neurons after brachial plexus avulsion in mice.

On 1 dpi, we observed a rapidly enhanced concentration of CXCL1 in the injured spinal cord. Studies in mice have shown that CXCL1 reduces the severity of multiple sclerosis and can exhibit a neuroprotective function. The concurrence of CXCR2(the receptor for CXCL1) on oligodendrocytes and induced CXCL1 on hypertrophic astrocytes in MS provides a novel mechanism for recruitment of oligodendrocytes to areas of damage, an essential prerequisite for lesion repair in this devastating condition. [41][42]. CXCL1 of might be actively involved in the regenerative processes in the CNS by recruiting oligodendrocytes to the injured spinal cord on the first 1 day after BPRA.

CD93 is a type I transmembrane glycoprotein that is expressed on the surface of platelets, and myeloid, endothelial, hematopoietic stem and natural killer cells. CD93 is strongly associated with immune cell phagocytosis, which regulates innate immunity and inflammation [51]. CD93 deletion also induces phagocyte impairment on scavenging apoptotic cells[52]. Our study found CD93 IR was low in the contralateral side of spinal cord, but increased during inflammatory reaction in the ipsilateral side of spinal cord, reaching a peak at early stage of BPRA and showing distinct cytoplasmic and nuclear

staining. These findings suggest that the CD93 cytoplasmic tail is mainly expressed in cell membranes yet may migrate towards the cytoplasm or nucleus with increasing inflammatory reaction.

The levels of the ICAM1 gradually increased with a peak reached on 14 day. As a cell-surface glycoprotein typically expressed by both immune system cells and endothelial cells. ICAM1 is also expressed by astrocytes, though at low levels in resting, quiescent astrocytes, remarkably it is induced 12-fold following injury and subsequent astrocyte activation [53]. ICAM1 may facilitate astrocyte-lymphocyte interactions ultimately aiding recruitment of immune cells into the CNS [54].

Conclusions

In our study, we evaluated the cytokine profile in spinal cord of mice with a model of BPRA in acute and subacute periods after injury. Our study also demonstrated that the MNs degeneration process, inflammatory reaction and immunological response after BPRA. A further study of a complex cytokine network imbalance after BPRA and determining its possible correlation with the severity of damage and clinical events seems important. This would provide a better understanding of the role cytokines play in the pathophysiology of the BPRA disease.

Abbreviations

BPRA, brachial plexus root avulsion; MNs, Motoneurons; CNS, central nervous system; TEM, transmission electron microscopy; dpi, day post injury

Declarations

Acknowledgements

The authors acknowledge the general support provided by Yaqiong Wang for her professional assistance in the tissue process and electron microscope observation.

Authors' contributions

ZK designed this study, performed the experiments and drafted the manuscript. LYQ and TY carried out extra data analysis. YGY and PRINCE participated in drafting and revised the manuscript. ZYY and XXY revised the manuscript, FR and ZLH supervised the design of the study and conceived the manuscript. All authors reviewed and approved the final version of this paper.

Funding

This study was supported by the National Natural Science Foundation of China, No. 81771325; the Natural Science Foundation of Guangdong Province of China, No. 2016A030310224; Young Teacher Foundation of Sun Yat-sen University, No. 59000-18841219

Availability of data and materials

The datasets used and/or analyzed during the current study are available from the corresponding author on reasonable request.

Ethics approval

All animal experiments were approved by the Animal Care and Use Committee of Sun Yat-sen University and the Guangdong Province Animal Care Ethics Committee.

Consent for publication

Not applicable.

Competing interests

The authors declare that they have no competing interests.

References

1. 10.1016/j.neuroscience.2019.01.054
   Chen S, Hou Y, Zhao Z, Luo Y, Lv S, Wang Q, et al. Neuregulin-1 Accelerates Functional Motor Recovery by Improving Motoneuron Survival After Brachial Plexus Root Avulsion in Mice. Neuroscience [Internet]. IBRO; 2019;404:510–8. Available from: https://doi.org/10.1016/j.neuroscience.2019.01.054.
2. Chu T-H, Wu W. Neurotrophic Factor Treatment After Spinal Root Avulsion Injury. Cent Nerv Syst Agents Med Chem. 2011;9:40–55.
3. Yakovlev AG, Faden AI. Mechanisms of Neural Cell Death: Implications for Development of Neuroprotective Treatment Strategies. NeuroRx. 2004;1:5–16.
4. 10.1016/j.freeradbiomed.2019.08.029
   Zhang X, Liu XD, Xian YF, Zhang F, Huang PY, Tang Y, et al. Berberine enhances survival and axonal regeneration of motoneurons following spinal root avulsion and re-implantation in rats. Free Radic Biol Med [Internet]. Elsevier B.V.; 2019;143:454–70. Available from: https://doi.org/10.1016/j.freeradbiomed.2019.08.029.
5. Ali ZS, Johnson VE, Stewart W, Zager EL, Xiao R, Heuer GG, et al. Neuropathological characteristics of brachial plexus avulsion injury with and without concomitant spinal cord injury. J Neuropathol Exp Neurol. 2016;75:69–85.
6. 10.1038/s41598-019-48003-9
   Zhou Z, Huang G, xiang, Lu J, Ma J, Yuan Q jun, Cao Y, et al. Up-regulation of heat shock protein 27 inhibits apoptosis in lumbosacral nerve root avulsion-induced neurons. Sci Rep [Internet]. Springer US; 2019;9:1–10. Available from: http://dx.doi.org/10.1038/s41598-019-48003-9.

7. Barbizan R, Oliveira ALR. Impact of acute inflammation on spinal motoneuron synaptic plasticity following ventral root avulsion. J Neuroinflammation. 2010;7:1–16.
8. Gris D, Marsh DR, Oatway MA, Chen Y, Hamilton EF, Dekaban GA, et al. Transient Blockade of the CD11d/CD18 Integrin Reduces Secondary Damage after Spinal Cord Injury, Improving Sensory, Autonomic, and Motor Function. J Neurosci. 2004;24:4043–51.
9. Rice T, Larsen J, Rivest S, Yong VW. Characterization of the early neuroinflammation after spinal cord injury in mice. J Neuropathol Exp Neurol. 2007;66:184–95.
10. Olsson T, Piehl F, Swanberg M, Lidman O. Genetic dissection of neurodegeneration and CNS inflammation. J Neurol Sci. 2005;233:99–108.
11. Yuan Q, Xie Y, So KF, Wu W. Inflammatory response associated with axonal injury to spinal motoneurons in newborn rats. Dev Neurosci. 2003;25:72–8.
12. 10.1186/s41232-016-0026-1
Okada S. The pathophysiological role of acute inflammation after spinal cord injury. Inflamm Regen [Internet]. Inflammation and Regeneration; 2016;36:1–7. Available from: http://dx.doi.org/10.1186/s41232-016-0026-1.
13. 10.1016/j.brainres.2014.12.045
Gensel JC, Zhang B. Macrophage activation and its role in repair and pathology after spinal cord injury. Brain Res [Internet]. Elsevier; 2015;1619:1–11. Available from: http://dx.doi.org/10.1016/j.brainres.2014.12.045.
14. Zhou Y, Guo W, Zhu Z, Hu Y, Wang Y, Zhang X, et al. Macrophage migration inhibitory factor facilitates production of CCL5 in astrocytes following rat spinal cord injury. J Neuroinflammation Journal of Neuroinflammation. 2018;15:1–12.
15. Thomas DR, Wilson MM, Wigmore SJ, Moses AG, Filippatos GS, Gheorghiade M, et al. A Pericyte Origin of Spinal. Science. 2011;333:238–43.
16. Leon S, Yin Y, Nguyen J, Irwin N, Benowitz LI. Lens injury stimulates axon regeneration in the mature rat optic nerve. J Neurosci. 2000;20:4615–26.
17. Yin Y, Henzl MT, Lorber B, Nakazawa T, Thomas TT, Jiang F, et al. Oncomodulin is a macrophage-derived signal for axon regeneration in retinal ganglion cells. Nat Neurosci. 2006;9:843–52.
18. Mietto BS, Kroner A, Girolami EI, Santos-Nogueira E, Zhang J, David S. Role of IL-10 in resolution of inflammation and functional recovery after peripheral nerve injury. J Neurosci. 2015;35:16431–42.
19. Bruce M, Streifel KM, Boosalis CA, Heuer L, González EA, Li S, et al. Acute peripheral immune activation alters cytokine expression and glial activation in the early postnatal rat brain. J Neuroinflammation Journal of Neuroinflammation. 2019;16:1–15.
20. Sato A, Ohtaki H, Tsumuraya T, Song D, Ohara K, Asano M, et al. Interleukin-1 participates in the classical and alternative activation of microglia/macrophages after spinal cord injury. J Neuroinflammation. 2012;9:1–17.
21. Fenn AM, Hall JCE, Gensel JC, Popovich PG, Godbout JP. IL-4 signaling drives a unique arginase+/IL-1β + microglia phenotype and recruits macrophages to the inflammatory CNS: Consequences of age-

related deficits in IL-4Rα after traumatic spinal cord injury. J Neurosci. 2014;34:8904–17.

22. Gharagozloo M, Kalantari H, Rezaei A, Maracy MR, Salehi M, Bahador A, et al. CLINICAL STUDY Immune-mediated cochleovestibular disease. Bratisl lek??rske List. 2015;116:296–301.
23. Senturk S, Yaman ME, Aydin HE, Guney G, Bozkurt I, Paksoy K, et al. Effects of resveratrol on inflammation and apoptosis after experimental spinal cord injury. Turk Neurosurg. 2018;28:889–96.
24. Sun L, Li M, Ma X, Feng H, Song J, Lv C, et al. Inhibition of HMGB1 reduces rat spinal cord astrocytic swelling and AQP4 expression after oxygen-glucose deprivation and reoxygenation via TLR4 and NF-KB signaling in an IL-6-dependent manner. J Neuroinflammation Journal of Neuroinflammation. 2017;14:1–18.
25. Liu Y, Zhou LJ, Wang J, Li D, Ren WJ, Peng J, et al. TNF-α differentially regulates synaptic plasticity in the hippocampus and spinal cord by microglia-dependent mechanisms after peripheral nerve injury. J Neurosci. 2017;37:871–81.
26. Abdullah A, Zhang M, Frugier T, Bedoui S, Taylor JM, Crack PJ. STING-mediated type-I interferons contribute to the neuroinflammatory process and detrimental effects following traumatic brain injury. J Neuroinflammation Journal of Neuroinflammation. 2018;15:1–17.
27. Losey P, Young C, Krimholtz E, Bordet R, Anthony DC. The role of hemorrhage following spinal-cord injury. Brain Res. 2014;1569:9–18.
28. Garcia E, Aguilar-Cevallos J, Silva-Garcia R, Ibarra A. Cytokine and growth factor activation in vivo and in vitro after spinal cord injury. Mediators Inflamm. Hindawi Publishing Corporation; 2016;2016.
29. Zhu P, Li JX, Fujino M, Zhuang J, Li XK. Development and treatments of inflammatory cells and cytokines in spinal cord ischemia-reperfusion injury. Mediators Inflamm. 2013;2013.
30. Pranzatelli MR. Advances in biomarker-guided therapy for pediatric- and adult-onset neuroinflammatory disorders: Targeting chemokines/cytokines. Front Immunol. 2018;9.
31. Nicol LSC, Thornton P, Hatcher JP, Glover CP, Webster CI, Burrell M, et al. Central inhibition of granulocyte-macrophage colony-stimulating factor is analgesic in experimental neuropathic pain. Pain. 2018;159:550–9.
32. 10.1016/j.neuint.2019.104611
    Yu G, Zilundu PLM, Xu X, Li Y, Zhou Y, Zhong K, et al. The temporal pattern of brachial plexus root avulsion-induced lncRNA and mRNA expression prior to the motoneuron loss in the injured spinal cord segments. Neurochem Int [Internet]. Elsevier; 2020;132:104611. Available from: https://doi.org/10.1016/j.neuint.2019.104611.
33. Li Y, Song F, huan, Zhong K, Yu G, yin, Zilundu PLM, Zhou Y, ying, et al. Pre-Injection of Small Interfering RNA (siRNA) Promotes c-Jun Gene Silencing and Decreases the Survival Rate of Axotomy-Injured Spinal Motoneurons in Adult Mice. J Mol Neurosci Journal of Molecular Neuroscience. 2018;65:400–10.
34. Yu G, Zilundu P, Liu L, Zhong K, Tang Y, Ling Z, et al. ERRγ is downregulated in injured motor neuron subpopulations following brachial plexus root avulsion. Exp Ther Med. 2019;205–13.
35. 10.1016/j.niox.2018.01.008

Tang Y, Fu R, Ling ZM, Liu L, lin, Yu G yin, Li W, et al. MiR-137–3p rescue motoneuron death by targeting calpain-2. Nitric Oxide - Biol Chem [Internet]. Elsevier; 2018;74:74–85. Available from: https://doi.org/10.1016/j.niox.2018.01.008.

36. Zhou LH, Han S, Xie YY, Wang LL, Yao Z, Bin. Differences in c-jun and nNOS expression levels in motoneurons following different kinds of axonal injury in adult rats. Brain Cell Biol. 2008;36:213–27.
37. 10.1016/j.niox.2009.11.005
    Wang J, Yan L, Zhao X, Wu W, Zhou LH. The diversity of nNOS gene expression in avulsion-injured spinal motoneurons among laboratory rodents. Nitric Oxide - Biol Chem [Internet]. Elsevier Inc.; 2010;22:37–42. Available from: http://dx.doi.org/10.1016/j.niox.2009.11.005.
38. Cheng X, Fu R, Gao M, Liu S, Li YQ, Song FH, et al. Intrathecal application of short interfering RNA knocks down c-jun expression and augments spinal motoneuron death after root avulsion in adult rats. Neuroscience. 2013;241:268–79.
39. Mukhamedshina YO, Akhmetzyanova ER, Martynova EV, Khaiboullina SF, Galieva LR, Rizvanov AA. Systemic and local cytokine profile following spinal cord injury in rats: A multiplex analysis. Front Neurol. 2017;8:1–7.
40. Wu X, Wittwer AJ, Carr LS, Crippes BA, DeLarco JE, Lefkowith JB. Cytokine-induced neutrophil chemoattractant mediates neutrophil influx in immune complex glomerulonephritis in rat. J Clin Invest. 1994;94:337–44.
41. 10.1016/j.mad.2019.111147
    Revuelta M, Elicegui A, Moreno-Cugnon L, Bührer C, Matheu A, Schmitz T. Ischemic stroke in neonatal and adult astrocytes. Mech Ageing Dev [Internet]. Elsevier; 2019;183:111147. Available from: https://doi.org/10.1016/j.mad.2019.111147.
42. Omari KM, John G, Lango R, Raine CS. Role for CXCR2 and CXCL1 on glia in multiple sclerosis. Glia. 2006;53:24–31.
43. Trinchieri G. Interleukin-12: A Proinflammatory Cytokine with Immunoregulatory Functions that Bridge Innate Resistance and Antigen-Specific Adaptive Immunity. Annu Rev Immunol. 1995;13:251–76.
44. Lee JH, Kim B, Jin WJ, Kim HH, Ha H, Lee ZH. Pathogenic roles of CXCL10 signaling through CXCR3 and TLR4 in macrophages and T cells: Relevance for arthritis. Arthritis Res Ther Arthritis Research Therapy. 2017;19:1–14.
45. Krauthausen M, Saxe S, Zimmermann J, Emrich M, Heneka MT, Müller M. CXCR3 modulates glial accumulation and activation in cuprizone-induced demyelination of the central nervous system. J Neuroinflammation. 2014;11:1–12.
46. Jiang BC, He LN, Wu XB, Shi H, Zhang WW, Zhang ZJ, et al. Promoted interaction of C/EBPα with demethylated Cxcr3 gene promoter contributes to neuropathic pain in mice. J Neurosci. 2017;37:685–700.
47. 10.1016/j.expneurol.2014.09.019

Guan XH, Fu QC, Shi D, Bu HL, Song ZP, Xiong BR, et al. Activation of spinal chemokine receptor CXCR3 mediates bone cancer pain through an Akt-ERK crosstalk pathway in rats. Exp Neurol [Internet]. Elsevier B.V.; 2015;263:39–49. Available from: http://dx.doi.org/10.1016/j.expneurol.2014.09.019.

48. Mojsilovic-Petrovic J, Callaghan D, Cui H, Dean C, Stanimirovic DB, Zhang W. Hypoxia-inducible factor-1 (HIF-1) is involved in the regulation of hypoxia-stimulated expression of monocyte chemoattractant protein-1 (MCP-1/CCL2) and MCP-5 (Ccl12) in astrocytes. J Neuroinflammation. 2007;4:1–15.
49. 10.1038/emboj.2010.256
Ren M, Guo Q, Guo L, Lenz M, Qian F, Koenen RR, et al. Polymerization of MIP-1 chemokine (CCL3 and CCL4) and clearance of MIP-1 by insulin-degrading enzyme. EMBO J [Internet]. Nature Publishing Group; 2010;29:3952–66. Available from: http://dx.doi.org/10.1038/emboj.2010.256.
50. McMahon EJ, Cook DN, Suzuki K, Matsushima GK. Absence of Macrophage-Inflammatory Protein-1α Delays Central Nervous System Demyelination in the Presence of an Intact Blood-Brain Barrier. J Immunol. 2001;167:2964–71.
51. Harhausen D, Prinz V, Ziegler G, Gertz K, Endres M, Lehrach H, et al. CD93/AA4.1: A Novel Regulator of Inflammation in Murine Focal Cerebral Ischemia. J Immunol. 2010;184:6407–17.
52. Greenlee MC, Sullivan SA, Bohlson SS. Detection and characterization of soluble CD93 released during inflammation. Inflamm Res. 2009;58:909–19.
53. Zamanian JL, Xu L, Foo LC, Nouri N, Zhou L, Giffard RG, et al. Genomic analysis of reactive astrogliosis. J Neurosci. 2012;32:6391–410.
54. Liddelow S, Hoyer D. Tet Operators. Curr Drug Targets [Internet]. 2016;17:156–67. Available from: https://www.ncbi.nlm.nih.gov/pmc/articles/PMC5070417/pdf/CGT-16-156.pdf.

Figures

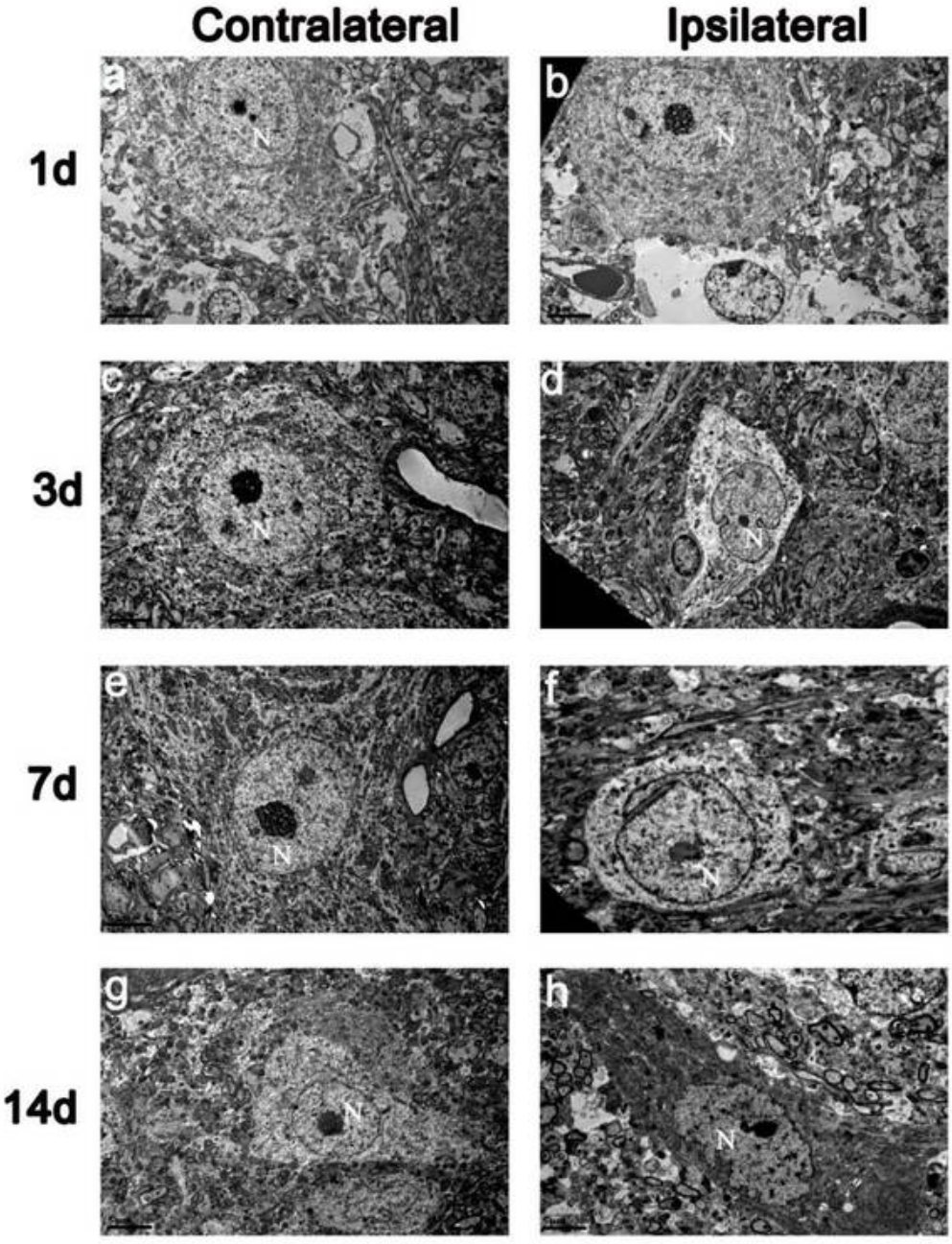
Contralateral
Ipsilateral
1d
3d
7d
14d
a
b
c
d
e
f
g
h
N

Figure 1

Electron microscopy (EM) photographs of motorneurons (MNs) after unilateral brachial plexus roots avulsion injury (BPRA) in mice. Representative EM microphotographs of spinal MNs at 1-14 days post-injury (dpi) of unilateral BPRA in adult mice. As compared to the MNs in the contralateral side ventral horn of injured spinal segment (a, c, e, and g), the injured MNs in the ipsilateral side show a mixed morphological feature of apoptosis and necrosis, reflected as a swollen and crenellated cellular shape and an inflated mitochondria at 1dpi (b). It was also noted that a dramatic reduction of organelles in the injured MNs cytoplasm with an irregular nuclear envelope at 3-7 dpi (d, f). Moreover, the nuclear materials demonstrated pyknotic by the 14 dpi (f). n=5 mice/group. Scale bar=5μm.N=nucleus.

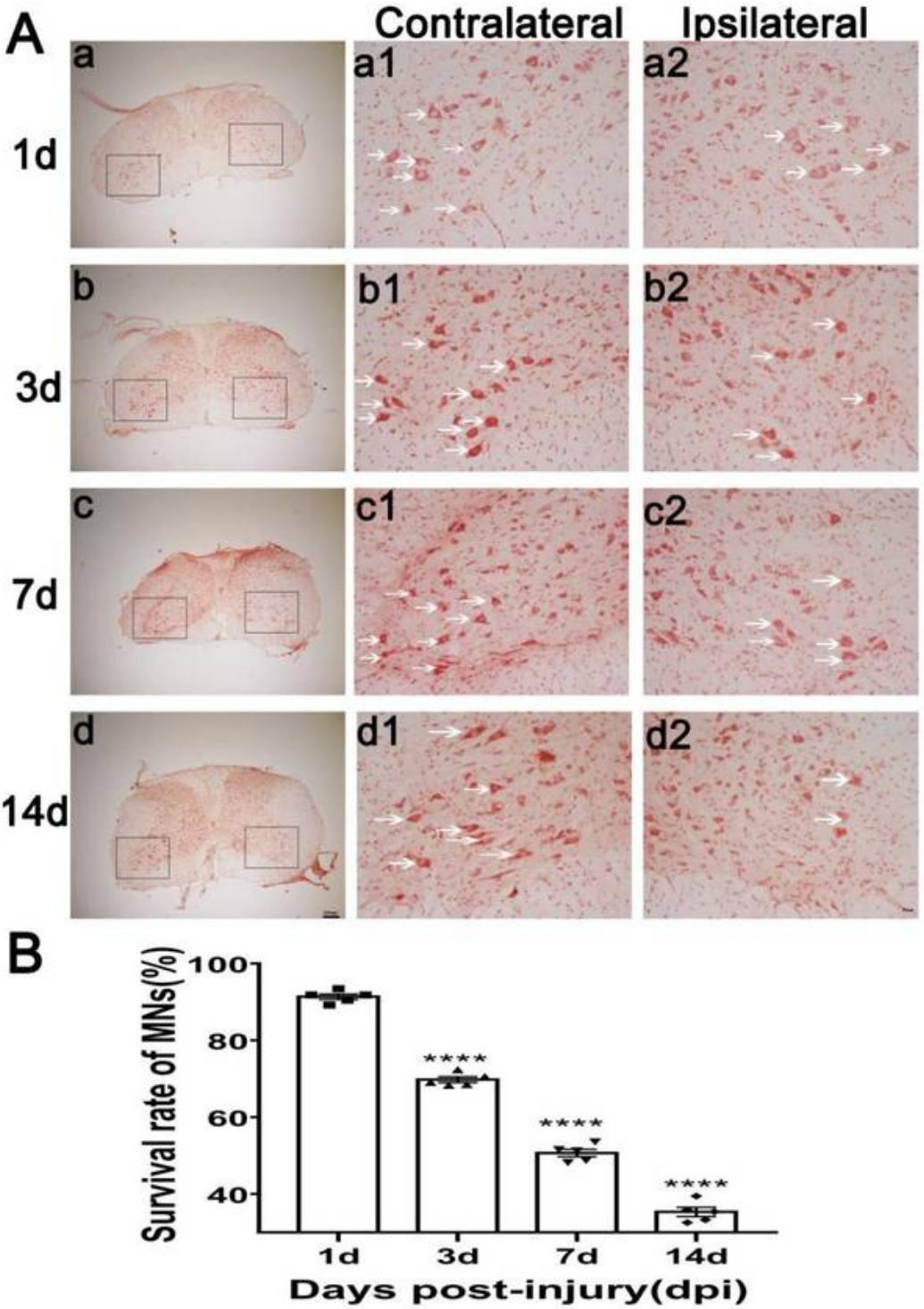
A
Contralateral
Ipsilateral
a
a1
a2
1d
b
b1
b2
3d
c
c1
c2
7d
d
d1
d2
14d
B
Survival rate of MNs(%)
100
80
60
40
****
****
****
1d
3d
7d
14d
Days post-injury(dpi)

Figure 2

Unilateral BPRA caused a dramatic motoneurons (MNs) loss in the ventral horn of the injured spinal cord. The spinal cord was harvested for cryostat, the 30μm section counterstained with neutral red at 1-14 days post-injury (dpi) to evaluate the MNs survival rate. Panel A is the representative microphotographs that depict the coronal section of spinal segments suffered from unilateral BPRA at 1-14 dpi (a-d). a1-d1, a2-d2 are representative images showing MNs in the contralateral (Con) and ipsilateral (Ipsi) ventral horn of the spinal cord (outlined in the rectangular area in a-d) respectively. Panel B summarizes the change of the MNs survival rate during 1-14 dpi. ****p< 0.0001 vs. 1d, One-way ANOVA followed by Tukey post hoc test, n=5 mice/group. All data were presented in mean ± S.E.M. The white arrow indicates motoneurons. Scale bar=200μm (a-d) or 50 μm (a1-d1, a2-d2).

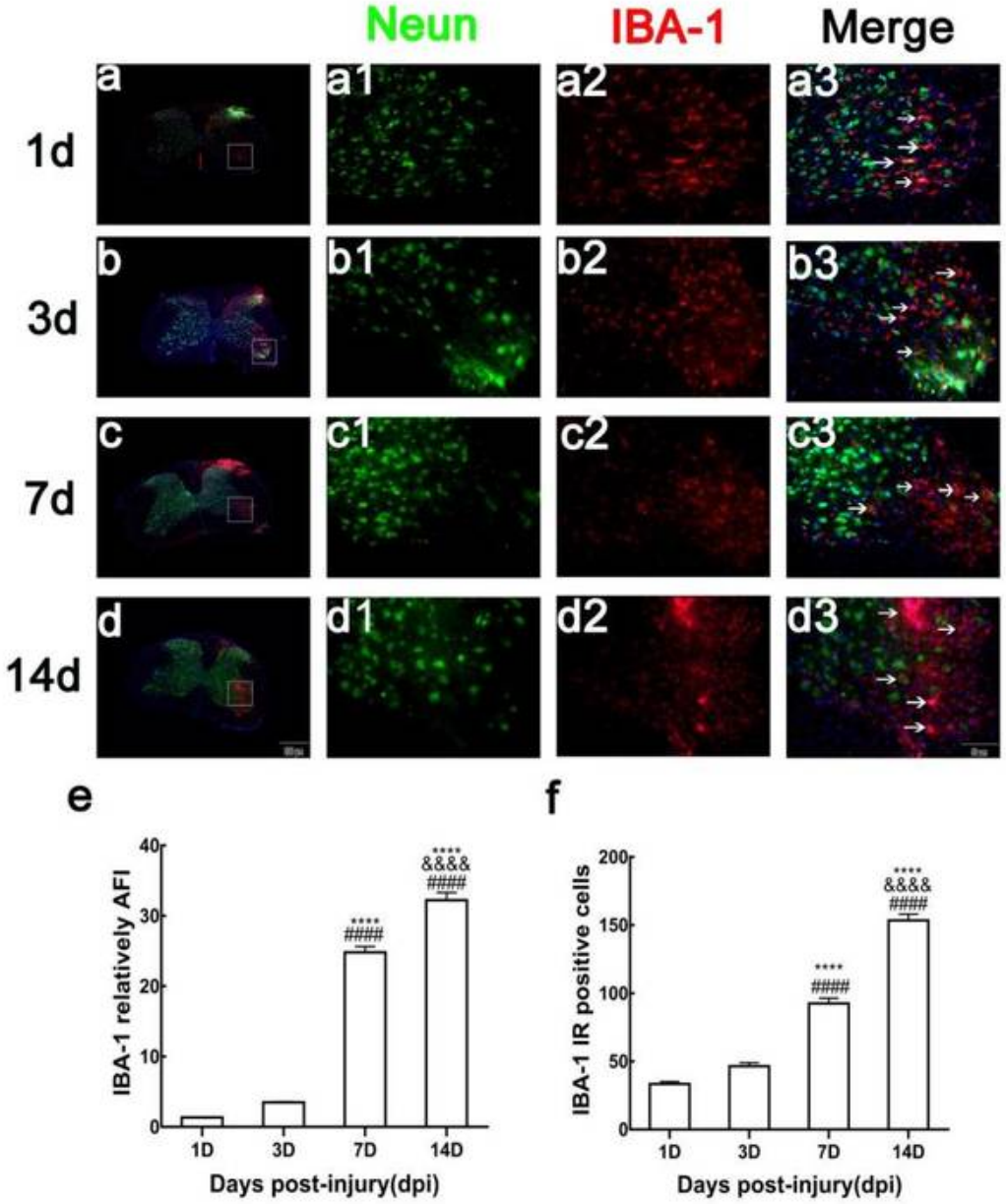
Neun
IBA-1
Merge
a
a1
a2
a3
1d
b
b1
b2
b3
3d
c
c1
c2
c3
7d
d
d1
d2
d3
14d
e
IBA-1 relatively AFI
40
30
20
10
0
1D
3D
7D
14D
Days post-injury(dpi)
****
####
&&&&
f
IBA-1 IR positive cells
200
150
100
50
0
1D
3D
7D
14D
Days post-injury(dpi)

Figure 3

Unilateral BPRA upregulated microglia expression in the ipsilateral ventral horn of the spinal cord. Upper panel a-d are representative microphotographs showing the double immunostaining of IBA-1(red colour) and NeuN (green colour) of the corresponding spinal segment. The rectangular areas focus the ipsilateral ventral horn, which was highlighted in images observed under high magnification (a1-d3) at 1-14 days post-injury (dpi). Panel e and f summarize the change of the IBA-1 relative average fluorescence intensity (AFI) and immunoreactivity (IR) positive cells in the ipsilateral ventral horn during 1-14 dpi. ****p< 0.0001 vs. 1d, ####p< 0.0001 vs. 3d, &&&&p< 0.0001 vs. 7d, One-way ANOVA followed by Tukey post hoc test, n=5 mice/group. All data were presented in mean ± S.E.M. The white arrow indicates microglia. Scale bar=200 μm (a-d) or 50 μm (a1-d3).

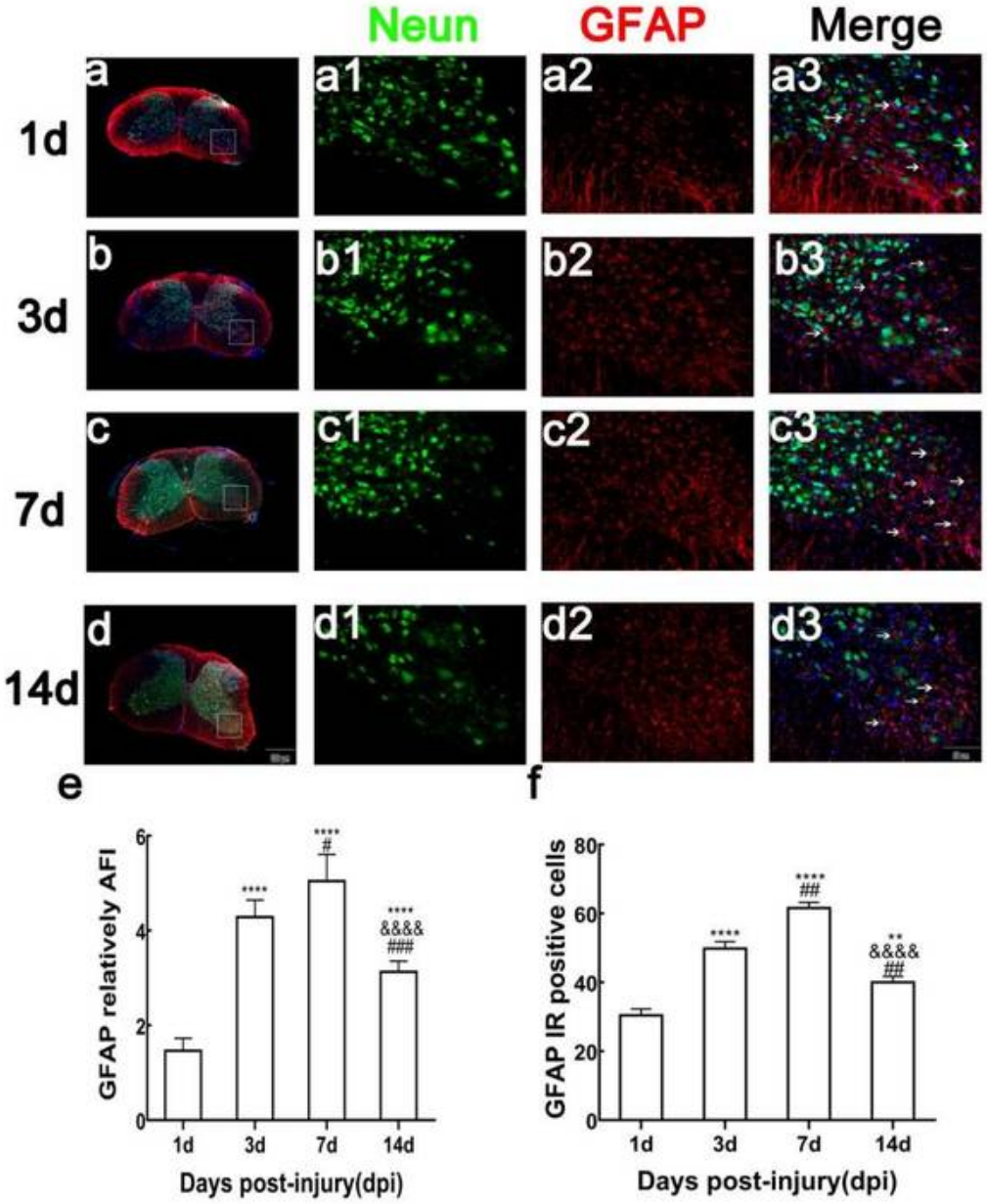
Neun
GFAP
Merge
1d
3d
7d
14d
a
a1
a2
a3
b
b1
b2
b3
c
c1
c2
c3
d
d1
d2
d3
e
f
GFAP relatively AFI
Days post-injury(dpi)
GFAP IR positive cells
Days post-injury(dpi)
1d
3d
7d
14d

Figure 4

BPRA activates astrocyte response in the ipsilateral ventral horn of the spinal cord. Upper panel a-d are representative microphotographs showing the double immunostaining of GFAP (red color) and NeuN (green color) of the corresponding spinal segment. The rectangular areas focus the ipsilateral ventral horn, which was highlighted in images observed under high magnification (a1-d3) at 1-14 days post-injury (dpi). Panel e and f summarize the change of the GFAP relative average fluorescence intensity (AFI) and immunoreactivity (IR) positive cells in the ipsilateral ventral horn during 1-14 dpi. ****p< 0.0001 vs. 1d, ####p< 0.0001 vs. 3d, &&&&p< 0.0001 vs. 7d, One-way ANOVA followed by Tukey post hoc test, n=5 mice/group. All data were presented in mean ± S.E.M. The white arrow indicates astrocyte. Scale bar=200 μm (a-d) or 50 μm (a1-d3).

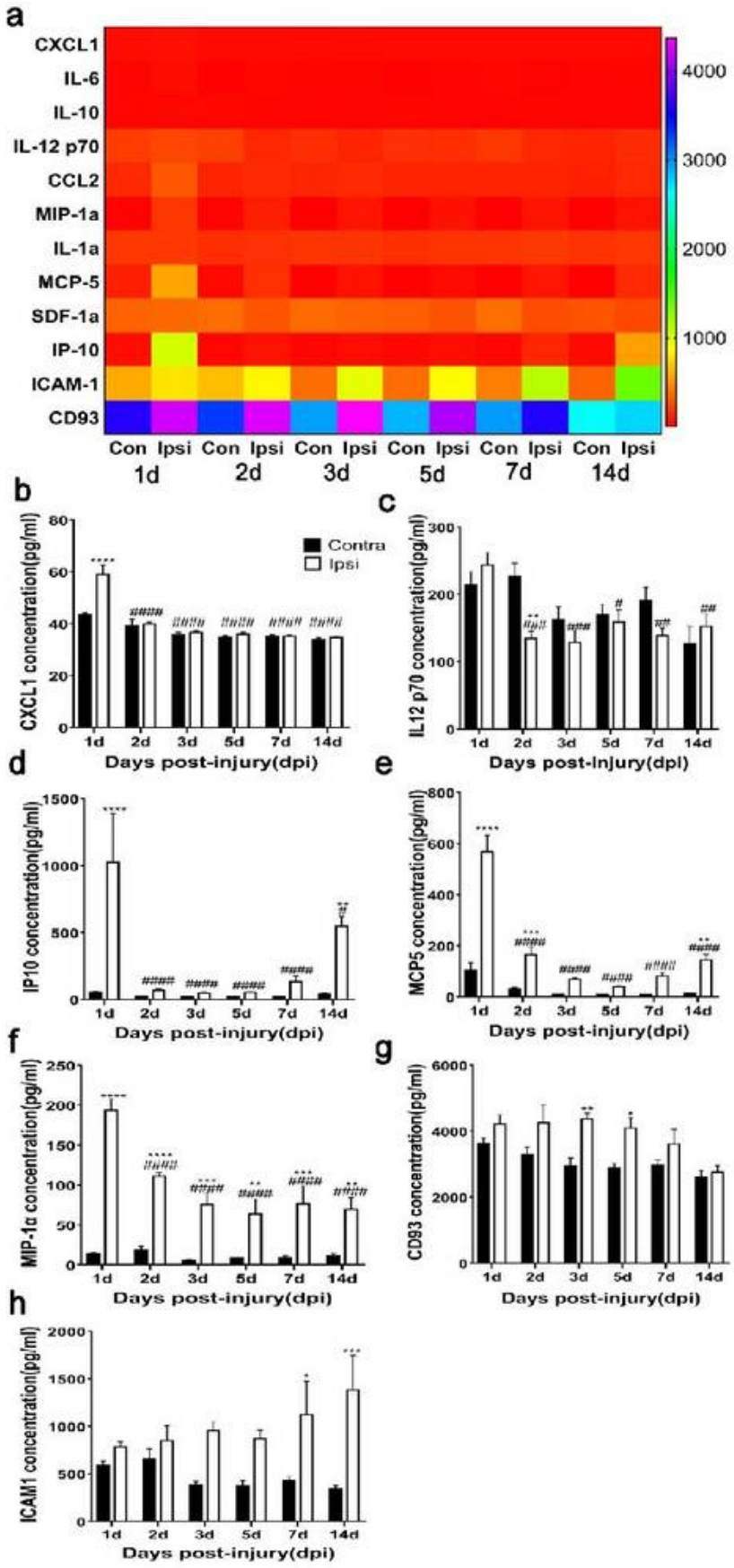
a
CXCL1
IL-6
IL-10
IL-12 p70
CCL2
MIP-1a
IL-1a
MCP-5
SDF-1a
IP-10
ICAM-1
CD93
4000
3000
2000
1000
Con Ipsi Con Ipsi Con Ipsi Con Ipsi Con Ipsi Con Ipsi
1d 2d 3d 5d 7d 14d
b
Contra
Ipsi
CXCL1 concentration(pg/ml)
Days post-injury(dpi)
c
IL12 p70 concentration(pg/ml)
Days post-injury(dpi)
d
IP10 concentration(pg/ml)
Days post-injury(dpi)
e
MCP5 concentration(pg/ml)
Days post-injury(dpi)
f
MIP-1α concentration(pg/ml)
Days post-injury(dpi)
g
CD93 concentration(pg/ml)
Days post-injury(dpi)
h
ICAM1 concentration(pg/ml)
Days post-injury(dpi)

Figure 5

The spinal cytokines level profile during the acute and subacute phase of BPRA injury. Upper panel showing a heat map analysis of 12 cytokines profile in contralateral and ipsilateral spinal cord at 1-14 days post unilateral BPRA injury in mice. Lower panel demonstrates the concentration (pg/ml) change of 7 significantly altered cytokines caused by the injury. ****p< 0.0001 vs. contralateral at each time point, ####p< 0.0001 vs. 1d within the ipsilateral group, Two-way ANOVA followed by Tukey post hoc test, n=6 mice/group.

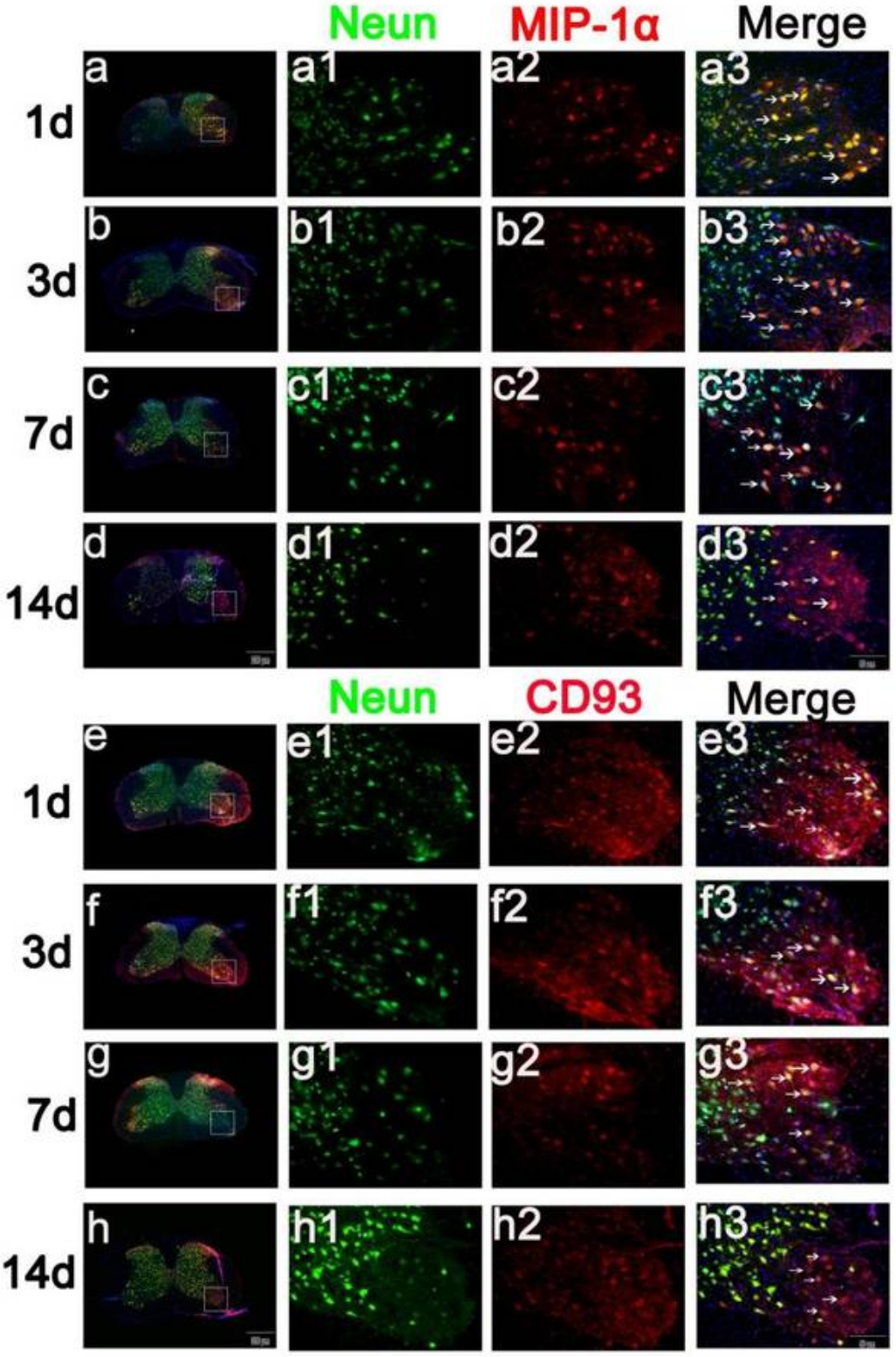
Neun
MIP-1α
Merge
a
a1
a2
a3
1d
b
b1
b2
b3
3d
c
c1
c2
c3
7d
d
d1
d2
d3
14d
Neun
CD93
Merge
e
e1
e2
e3
1d
f
f1
f2
f3
3d
g
g1
g2
g3
7d
h
h1
h2
h3
14d

Figure 6

Unilateral BPRA injury elevated the expression of MIP-1α and CD93 in the spinal cord. a-d shows the representative photomicrographs of MIP-1α expression in the spinal cord after 1-14 days after avulsion injury. The rectangular areas in a-d were further magnified to demonstrate the colocalization of NeuN (green colour,a1-d1) and MIP-1α (red colour, a2-d2) positive cells in the ipsilateral ventral horn. e-h shows the representative photomicrographs of CD93 expression in the spinal cord after 1-14 days after avulsion injury. The rectangular areas in a-d were further magnified to demonstrate the colocalization of NeuN (green colour,e1-h1) and CD93 (red colour, e2-h2) positive cells in the ipsilateral ventral horn. The white arrow indicates double immunostaining cells. Scale bar=200 μm (a-h) or 50 μm (a1-h3).

Supplementary Files

This is a list of supplementary files associated with this preprint. Click to download.

- SupplementarymaterialsTable1.docx